

# **Search for Defocusing During a Single Pulse of a 2 kA Relativistic Electron Beam due to Ions Accelerated from a Target**

*E.J. Lauer, G.J. Caporaso, F.W. Chambers, Y.-J. Chen,  
S. Falabella, G. Guethlein, J. McCarrick, R. Richardson,  
S. Sampayan, J. Weir*

**September 5, 2002**

**U.S. Department of Energy**

Lawrence  
Livermore  
National  
Laboratory



## DISCLAIMER

This document was prepared as an account of work sponsored by an agency of the United States Government. Neither the United States Government nor the University of California nor any of their employees, makes any warranty, express or implied, or assumes any legal liability or responsibility for the accuracy, completeness, or usefulness of any information, apparatus, product, or process disclosed, or represents that its use would not infringe privately owned rights. Reference herein to any specific commercial product, process, or service by trade name, trademark, manufacturer, or otherwise, does not necessarily constitute or imply its endorsement, recommendation, or favoring by the United States Government or the University of California. The views and opinions of authors expressed herein do not necessarily state or reflect those of the United States Government or the University of California, and shall not be used for advertising or product endorsement purposes.

This work was performed under the auspices of the U. S. Department of Energy by the University of California, Lawrence Livermore National Laboratory under Contract No. W-7405-Eng-48.

This report has been reproduced directly from the best available copy.

Available electronically at <http://www.doc.gov/bridge>

Available for a processing fee to U.S. Department of Energy  
And its contractors in paper from  
U.S. Department of Energy  
Office of Scientific and Technical Information  
P.O. Box 62  
Oak Ridge, TN 37831-0062  
Telephone: (865) 576-8401  
Facsimile: (865) 576-5728  
E-mail: [reports@adonis.osti.gov](mailto:reports@adonis.osti.gov)

Available for the sale to the public from  
U.S. Department of Commerce  
National Technical Information Service  
5285 Port Royal Road  
Springfield, VA 22161  
Telephone: (800) 553-6847  
Facsimile: (703) 605-6900  
E-mail: [orders@ntis.fedworld.gov](mailto:orders@ntis.fedworld.gov)  
Online ordering: <http://www.ntis.gov/ordering.htm>

OR

Lawrence Livermore National Laboratory  
Technical Information Department's Digital Library  
<http://www.llnl.gov/tid/Library.html>





# Search for Defocusing During a Single Pulse of a 2 kA Relativistic Electron Beam due to Ions Accelerated from a Target

E. J. Lauer, G. J. Caporaso, F. W. Chambers, Y-J Chen, S. Falabella, G. Guethlein, J. McCarrick, R. Richardson, S. Sampayan, and J. Weir

## I- Introduction

The DARHT accelerator will deliver several intense relativistic electron beam pulses to an x-ray conversion target during a few microseconds. Plasma from the target can cause a partial neutralization of the vacuum self-Er field resulting in an unacceptably large beam radius at the target. The Livermore group has been developing barrier foils to block the plasma from moving upstream. Positive ions accelerated upstream from the foil in the self-Ez field during a single pulse could defocus the beam. In May, 2001 LANL used a sensitive "two foil" experiment to search for such effects. They measured significant time dependent effects using conducting foils (1). In January, 2002, the Livermore group repeated the experiment using the ETA II accelerator. We expected to see similar effects and planned to collect data that we could model. We saw no significant effect from conducting foils unless the beam radius was small enough to damage the foil. The reason for the different results has not been explained and is still being investigated. Possibilities have to do with the longer pulse length at LANL, (60 ns compared to 40) or with the higher energy at LANL, (20 Mev compared to 5.7)

We also did some tests on dielectric targets where there is a strong effect to test our techniques.

A short summary of this report was presented at a conference (2).

## II-Apparatus

ETA II is an induction linear accelerator that produces 2 kA pulses of 5.7 Mev electrons. The energy is constant within 0.5 % during 40 ns. Fig 1 shows the apparatus used in these tests. Most of the tests were "two foil" experiments with the beam passing through a thin upstream foil and the time dependent beam radius measured on the downstream foil. We started with a set up with 33 cm between foils but the beam radius at the downstream foil was excessive and the foil separation was reduced to 17 cm. Some "single foil" measurements were also done with the upstream foil retracted and the beam passing through either a conducting or a non-conducting foil at the downstream location.

The most important measurements were made by imaging the light produced on the downstream foil onto a streak camera located outside the shield wall. A narrow slit was located at the entrance to the streak camera to form a beam profile and the profile light was streaked with the time axis perpendicular to the profile. The slit width was typically 0.1 cm and the time resolution was estimated to be 1.5 to 4 ns. In one test the slit was removed and the downstream foil was replaced by a thin quartz fiber. There was a graphite foil just upstream of the fiber. Cerenkov light from the fiber produced a beam profile which was imaged onto the streak camera. Framing camera images of the beam light from the two foils were also recorded.

The final magnetic focussing lens called C4 was centered 35 cm upstream of the first foil. In a typical run on a foil, we started with a low current in C4 and increased the

current in 10 or 20 A steps until either a hole was produced in the foil or a beam waist of 0.15 cm radius was produced at the foil. The currents in all the other lenses and steering coils were held constant. In one test the current in the next lens upstream of C4 called EF4 was reduced from 5 A to 3A and the current in C4 was increased to produce a 0.07 cm radius waist at the upstream foil.

The images acquired by the cameras are stored as electronic data files on computers. Our data reduction system starts with the beam profiles from the streak camera or from vertical and horizontal profiles generated from the framing camera images. A Gaussian shape is fitted to the profile data and the half width at half-maximum amplitude is the measured beam radius.

### III- Two Foil Experiments

Fig 2 shows a typical plot of beam radius at the upstream foil vs C4 current. A beam waist of 0.15 cm radius occurs at 360 A. The EF4 lens current was 5 A. This is for a conducting foil where there is no significant time dependence.

Fig 3 presents some curves generated using the beam envelope equation. The beam envelope equation is defined in Sect VI. The curve labeled "none" was produced by measuring the beam waist radius at the upstream foil to be 0.15 cm (with 360 A in C4) and then retracting the upstream foil and measuring a radius of 0.83 cm at the downstream foil. The emittance in the beam envelope equation was adjusted by trial and error to produce the curve to fit these measurements. The resulting emittance is  $7 \times 10^{-3}$  radian cm. Calculations are shown for each foil that was tested. For each curve an emittance of  $7 \times 10^{-3}$  was used for  $z < 0$  and a larger emittance calculated to result from foil scattering was used for  $z > 0$ . The radii at  $z = 17$  cm are the predictions in the absence of ion self force effects. Foil scattering was calculated using the formula of Williams (3):

$$\frac{d \langle \theta^2 \rangle}{dx} = \frac{8\pi e^4 n z (z+1)}{m^2 \gamma^2 \beta^4 c^4} \ln \frac{h z^{2/3} z^{1/2} n^{1/2}}{\pi^{1/2} m c \beta} \text{ cgs} \quad 1$$

where n is the number of atoms per cc of atomic number z and the other symbols have there usual meanings. We have also used

$$\epsilon_d = R \theta_d$$

$$\theta_d^2 = \theta_u^2 + \theta_s^2$$

$$\theta_u = \epsilon_u / R$$

where  $\epsilon$  is the emittance and u,d,s refer to upstream, downstream and scattering. The calculations are summarized in Table I.

Table I-Emittance After Passing Through Foils with R=0.15 cm Waist

FOIL	$\rho(\text{gm}/\text{cm}^3)$	$W(\text{gm}/\text{mole})$	$\epsilon_d(10^{-3} \text{ radcm})$
0.5 mil MYLAR $C_5O_2H_4$	1.4		7.37
2 mil KAPTAN $C_{22}H_{10}N_{205}$	1.43	3144	8.88
1 mil ALUMINUM	2.70	27	10.2
3 mil GRAPHITE	2.25	12.01	10.7
0.5 mil S STEEL	7.86	55.8	14.9
0.3 mil TANTALUM	16.6	181	25.6

In our experiments, the strength of single-pulse time-dependent focussing effects is strongly correlated with whether the target is a conductor or a non-conductor. Figs 4 through 14 are measurements from two-foil experiments on conductors; Fig 15 is a two-foil experiment on a non-conductor; Fig 16 is a one-foil experiment on a conductor and Figs 17 through 19 are one-foil results on a non-conductor.

Figs 4 and 5 are for a 1 mil aluminum upstream foil and are typical of all the results on conductors. Fig 4 presents the streak camera images as the C4 lens current is increased in small steps up to 361 A where we produce a 0.15 cm waist radius and a hole resulted. Fig 5 presents the corresponding downstream profile widths vs time. On the pulse where the foil was damaged, the beam radius at the downstream foil increased from about 1 cm to about 1.8 cm in 40 ns. For upstream beam radius  $>0.15$  cm there is no significant time dependence. Some of the foils were tested several times as we tried different techniques. On the figures of profile width vs time, we suggest that the most significant data is for the time range 50 to 100 ns; outside this range the beam current is too low.

The best streak data was obtained with a quartz downstream foil (25 mil thick) with tungsten evaporated onto the upstream side. The Cerenkov light from quartz was much brighter than the light from aluminum.

Fig 7 presents the results of a test where the downstream foil and slit system used for all the other cases was replaced by a quartz rod, (the system used at LANL). There was no significant difference in the results.

For Fig 9, the minimum beam radius on the upstream foil was 0.07 cm which may be compared with 0.15cm for all the other tests. This made no significant difference.

Fig 15 shows the results for a non-conducting upstream foil. As the spot size on the upstream foil is reduced, time dependence starts for about 0.5 cm radius and is very strong for 0.2 cm. Our model for the emission from dielectrics is that at the head of the beam the dielectric is a non conductor and there is a strong  $E_r$  and no  $E_z$ ;  $E_r$  is strong enough to cause electric breakdown over the surface of the dielectric with electrons avalanching outward. This creates a plasma which is a conductor and is also a source of ions.  $E_r$  switches off and  $E_z$  turns on accelerating ions.

#### IV-Single Foil Experiments

For these tests the upstream foil was retracted. Fig 16 gives results for a conductor. As the current in C4 is increased, the beam radius decreases and reaches a 0.2 cm waist for 309 A. There is no significant time dependence.

For Figs 17, 18 and 19 the graphite foil was removed and the beam hit bare quartz. For small current in C4, the radius starts large and decreases with time, eg at 234 A, R starts at 1.6 cm and decreases to 0.2 cm in 40 ns. For 309 A (which produces a 0.2 cm vacuum waist) the radius starts small and increases to about 1 cm in 40 ns. Fig 19 shows the framing camera images for 309 A for 5 times during the pulses.

#### V-Particle Model

The time dependent self-focusing associated with the strong ion emission when the beam hits a bare quartz foil (see Figs 17, 18, and 19) has been modeled using a PIC numerical calculation. The model assumes that there is an unlimited source of ion current density inside the time-zero beam edge radius at the target starting at time zero. Poisson's equation in r,z coordinates is solved with  $E_z=0$  at the target (space charge limited emission). The simulation domain in z is 33 cm long. The beam current is modeled with a 5 ns rise time. Simulations are done for H<sup>+</sup> and C<sup>+</sup> ions. Two curves on Fig 18 are simulated: C4=234A where the beam radius at the target increases with time and C4=309A where the radius decreases with time. Fig 20 shows the simulations for H<sup>+</sup> ions.  $t=0$  corresponds to 50 ns and  $t=50$  ns corresponds to 100 ns on Fig 18. The agreement between calculation and experiment is excellent. Fig 21 shows the simulations for C<sup>+</sup> ions. Singly charged ions this heavy can't move far enough during the beam pulse to explain the observations.

Figs 22 and 23 show the line density  $f$  vs  $z$  at 50 ns for, H<sup>+</sup> where  $f$  is the fractional neutralization of  $E_r$ . These curves show that the total ion emission current increases with decreasing beam size at the target.

#### VI-Modeling Ion Column Focusing Effects using the Beam Envelope Equation

Our beam envelope equation has an emittance term, a self-force term and a  $B_z$  term (4).

$$\frac{d^2 R}{dz^2} = \frac{\epsilon^2}{R^3} - \frac{(f - 1/\gamma^2)I(kA)}{(1 - 1/\gamma^2)\beta\gamma 17.05R} - k^2 R$$

2

$$k = \frac{eB_z}{2\beta\gamma mc^2}$$

where  $R$  is the rms beam radius,  $\epsilon$  is the rms emittance and  $f$  is the fractional neutralization of the beam self- $E_r$ .  $\epsilon$ ,  $f$  and  $k$  can be functions of  $z$ .  $\gamma$  is the beam electron total energy in rest-mass units and  $\beta$  is  $v_z/c$  for beam electrons where  $c$  is the velocity of light.  $e$  and  $m$  are the electron charge and rest mass in cgs esu.  $v_r/v_z \ll 1$  and there are no plasma electric currents. ETA II parameters are used

Figs 24 and 25 model two foil experiments starting with a time-zero beam envelope which has a 0.15 cm waist radius at the upstream foil, ( $z=0$ ), as used for most of the LLNL tests. The ion column is assumed to produce a constant  $f$  in a region extending

Calculations of space-charge-limited ion flow assuming an unlimited source (which may not be true), suggest that  $f$  is equal to or less than 0.4 (see Sect V); Fig 24 is for  $f=0.4$  and Fig 25 is for 0.2. C4 has 360A. An emittance increase at  $z=0$  for 1 mil aluminum was used, (that for 3 mil graphite is nearly the same. The curves suggest the following comments

1-As the column length increases, at first the waist moves a little downstream and the waist radius decreases and  $R[17]$  increases slightly; then the waist moves continually upstream.  $R[17]$  oscillates a little and then increases with increasing column length.

2-The largest effect is predicted to occur late in time.

3-Referring to Fig 5, 360A, the minimum effect that the LLNL experiment can reliably detect is for  $R[17]$  starting at 1cm and changing to 1.5. For  $R[0]<0.15$  cm we see no effect which implies that the ion column is weaker than that shown on Fig 25 with  $f=0.2$ ,  $Z=-32$  to 17 cm.

4-With a vacuum beam potential depression of 0.3 MV, protons can move about 32 cm in 40 ns (LLNL) or 48 cm in 60 ns LANL); no heavier ion can produce the required long column.

5- The longer pulse length at LANL may be the reason they see a bigger effect.

6- The sensitivity decreases with decreasing  $f$ .

Fig 26 is similar to Fig 25 except that it has a time-zero waist of 0.5 cm at the upstream foil.  $R$  is larger from  $z=0$  to  $-10.5$  and smaller beyond  $-10.5$ . The sensitivity is much less than that for a 0.15 cm waist.

Figs 27 and 28 model the strong effects seen in the single foil experiment on quartz,(see Figs 17, 18 and 19). Fig 27 is for C4=234A with  $R$  decreasing with time and Fig 28 is for 309A with  $R$  increasing with time. (These cases are also modeled in the particle modeling section.) For Fig 27, we have used the linearly decreasing  $f$  function found using the particle model. For Fig 28, we used a constant  $f=0.4$ . A smaller  $f$  would result in an excessive column length.

#### References:

1 H.A.Davis et al,Electron Beam Disruption due to Ion Release from Targets-Experimental Observations,14<sup>th</sup> International Conference on High Power Particle Beams,23-28 June,2002

2-E.J.Lauer et al,14<sup>th</sup> International Conference on High -Power Particle Beams,23-28 June,2002.

3-E. J. Williams, Proc. R. Soc. A 169, 542 (1939)

4-E. P. Lee and R. K. Cooper, Particle Accelerators, (1976), Vol. 7, 83-95

This work was performed under the auspices of the Department of Energy by the University of California, Lawrence Livermore National Laboratory under contract No W-7405-Eng-48

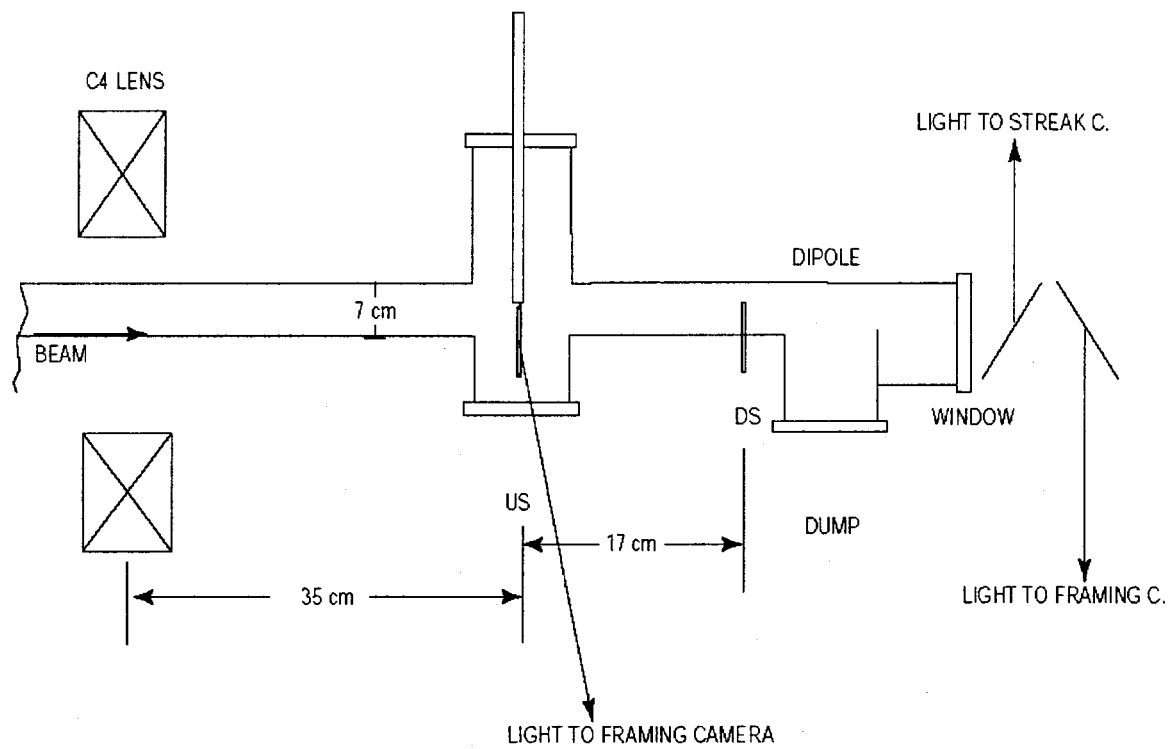


Fig 1-Schematic of Apparatus

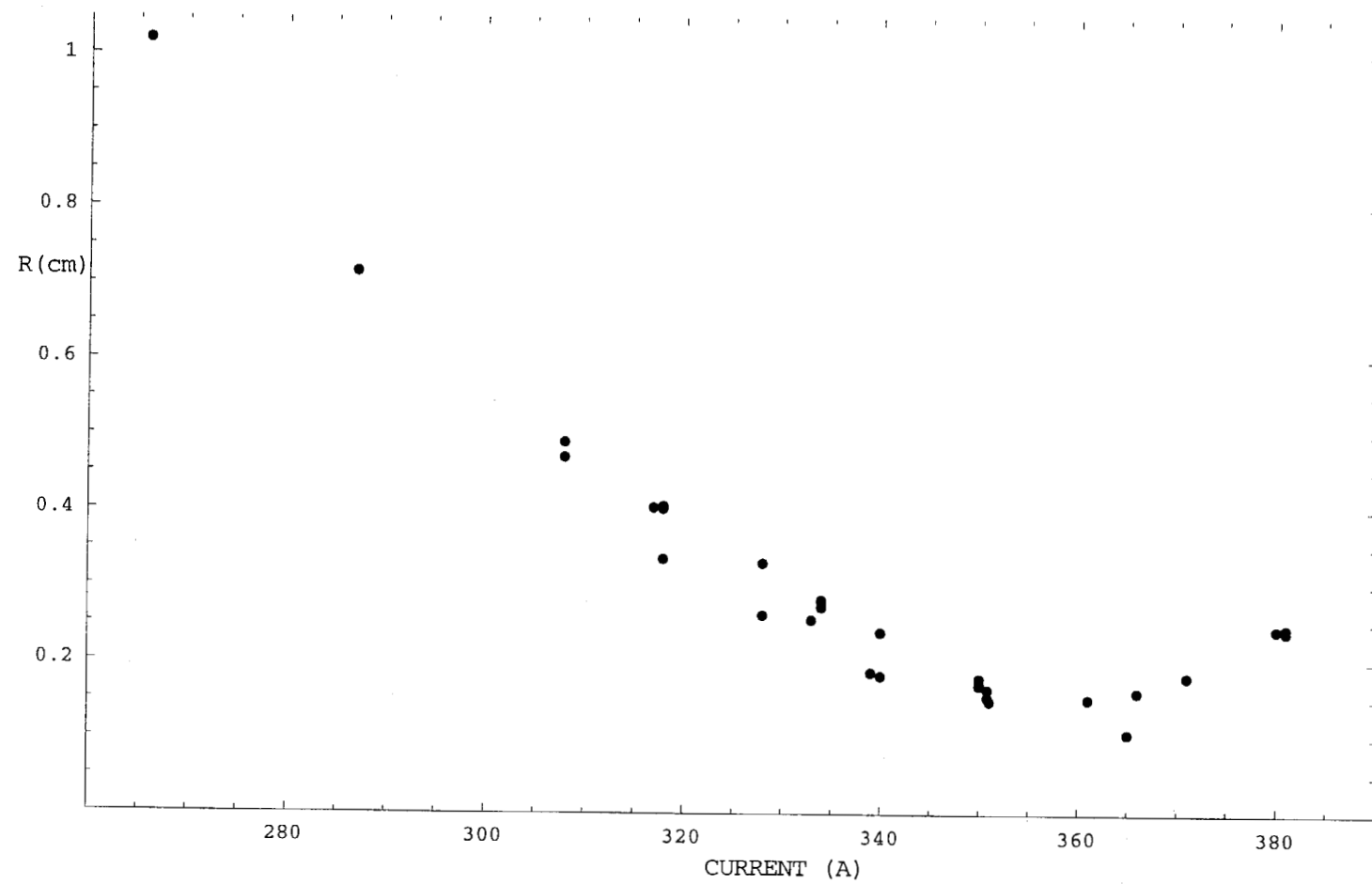


Fig 2 Beam Radius at First Foil vs C4 Lens Current (A), Graphite

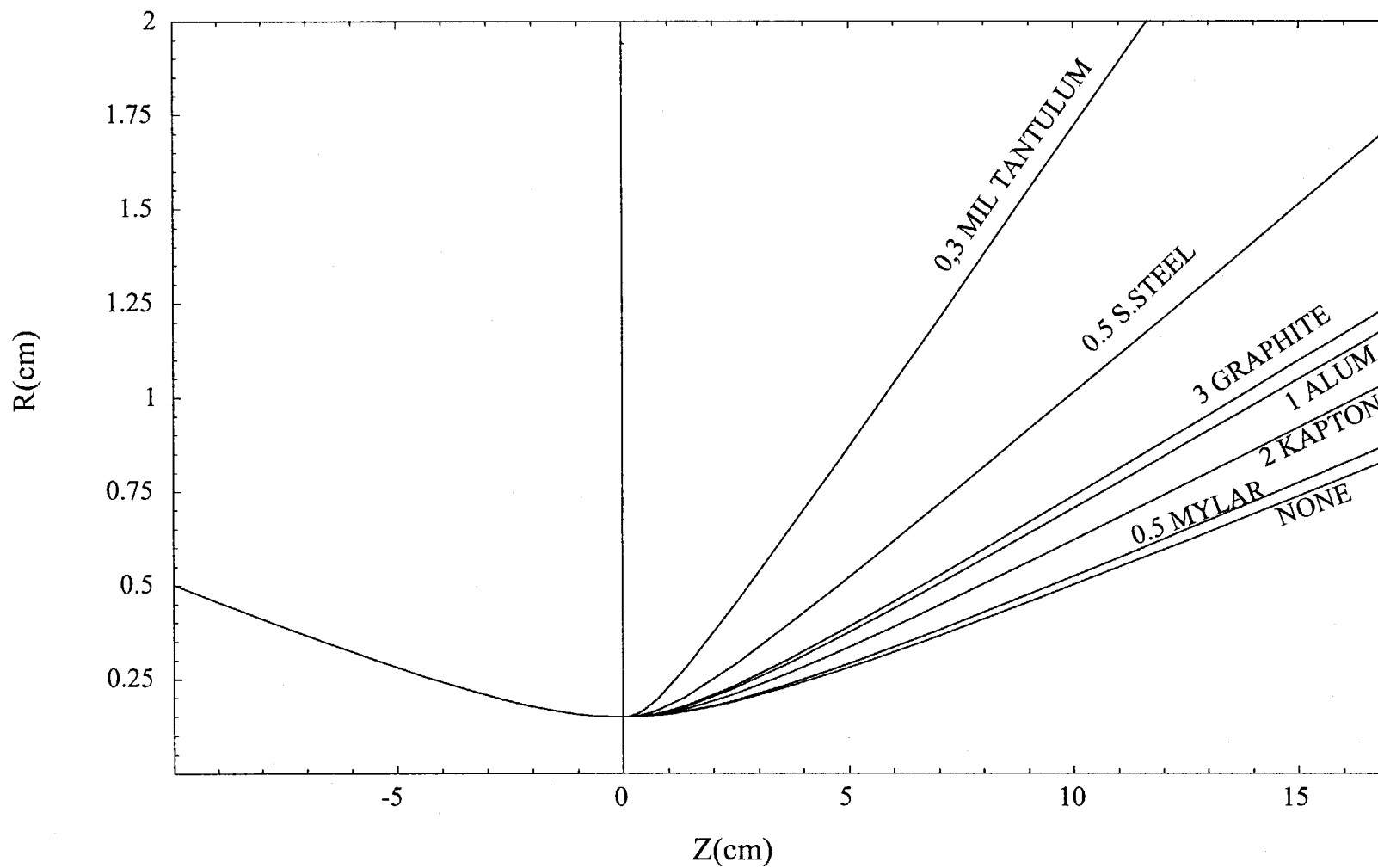


Fig 3 R vs Z showing the effect of foil scattering,  $f=0$  everywhere, C4  $Z_m=-35$  cm 360 A



### Streak camera images with C4 varied

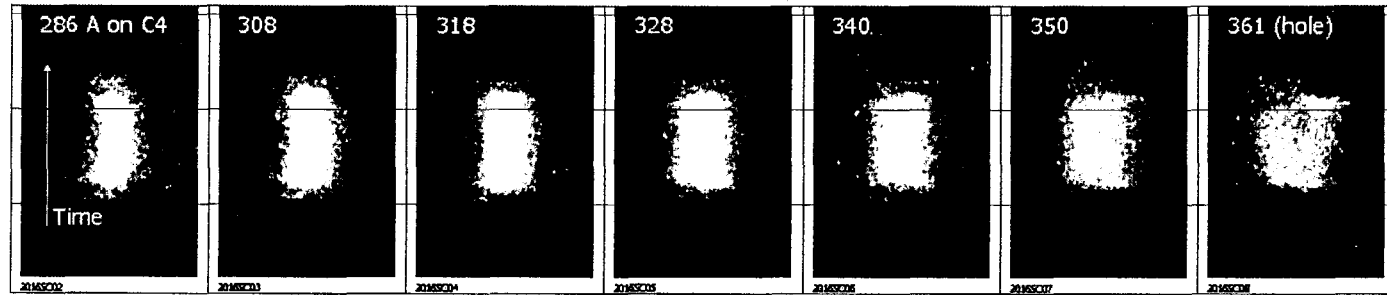


Fig 4-Upstream: 1 mil Aluminum, 0 (perpendicular to beam) & 38 degrees  
Downstream: 25 mil quartz w Tungsten on us (2022SCresults\_a005)

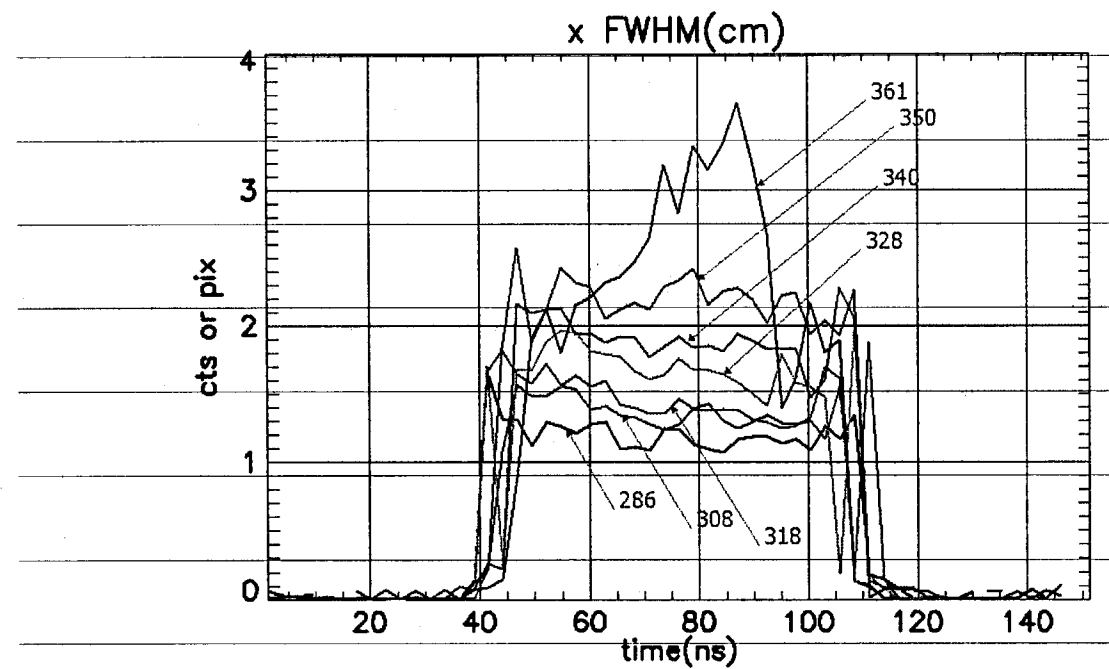


Fig 5 upstream: 1 mil aluminum rotated 38 degrees from perpendicular,  
downstream: 1 mil aluminum

File: 2022SCresults.std

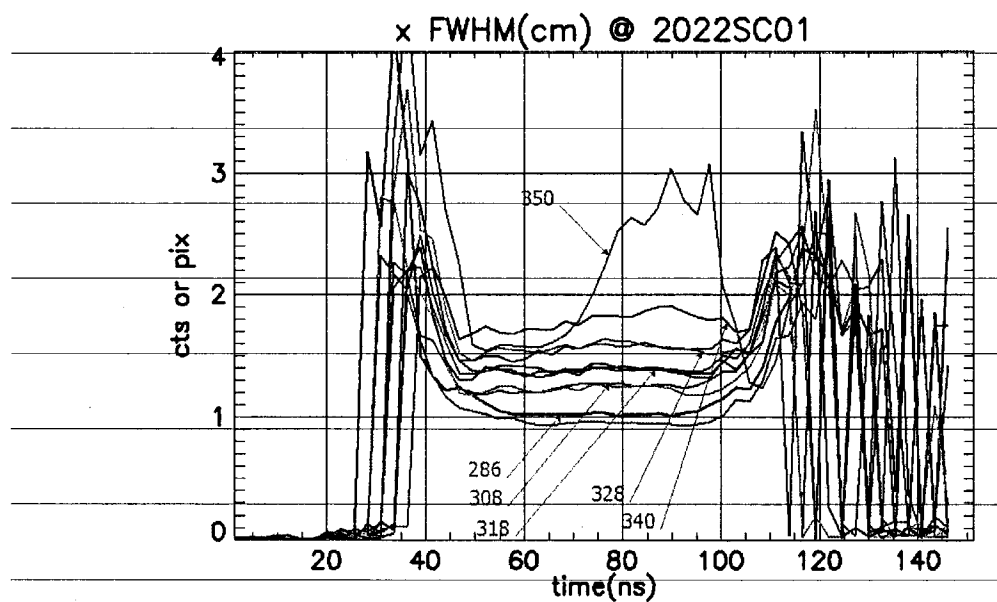


Fig 6 upstream: 1 mil aluminum 0 (perpendicular to beam) & 38 degrees  
downstream: 25-mil-quartz with tungsten on us side

2022SCresults.a005

File: 2031SC\_01to19.std

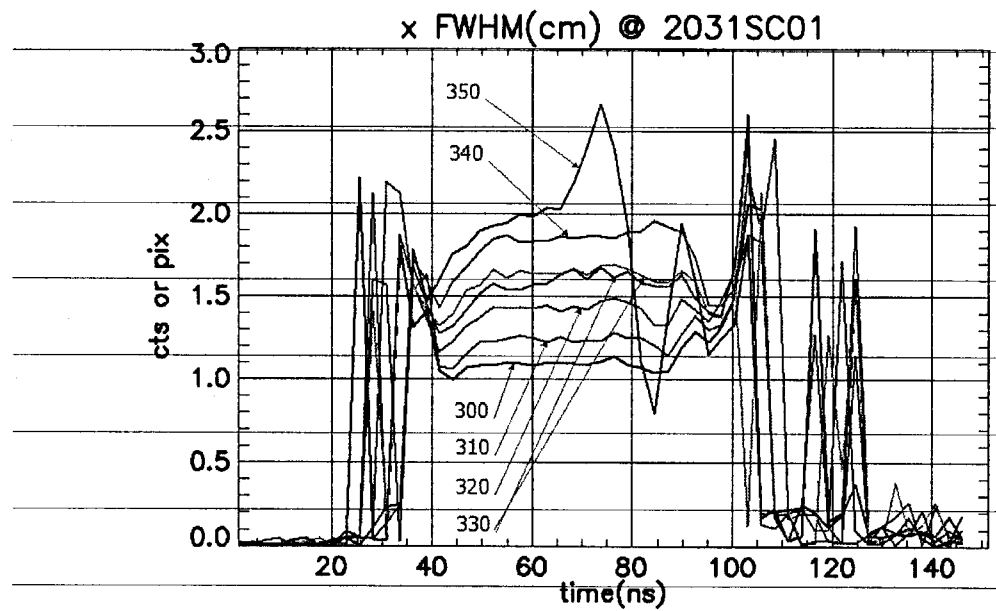


Fig 7 upstream: 3 mil graphite perpendicular to the beam  
downstream: 1 mm diam quartz rod, 3 mil graphite foil on us side

2031SC\_01to19\_a002

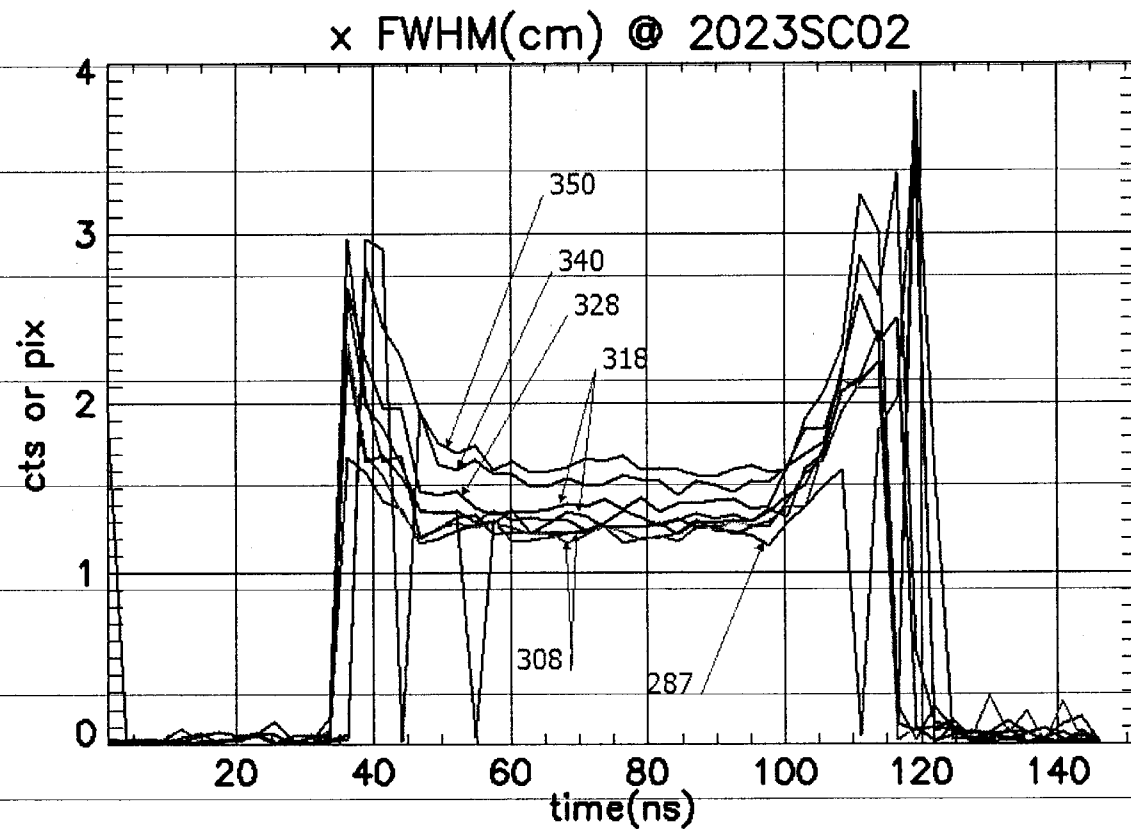


Fig 8 upstream: 3 mil graphite perpendicular to the beam  
downstream: 25 mil quartz with tungsten on us side

File: 2024SC01\_all.std

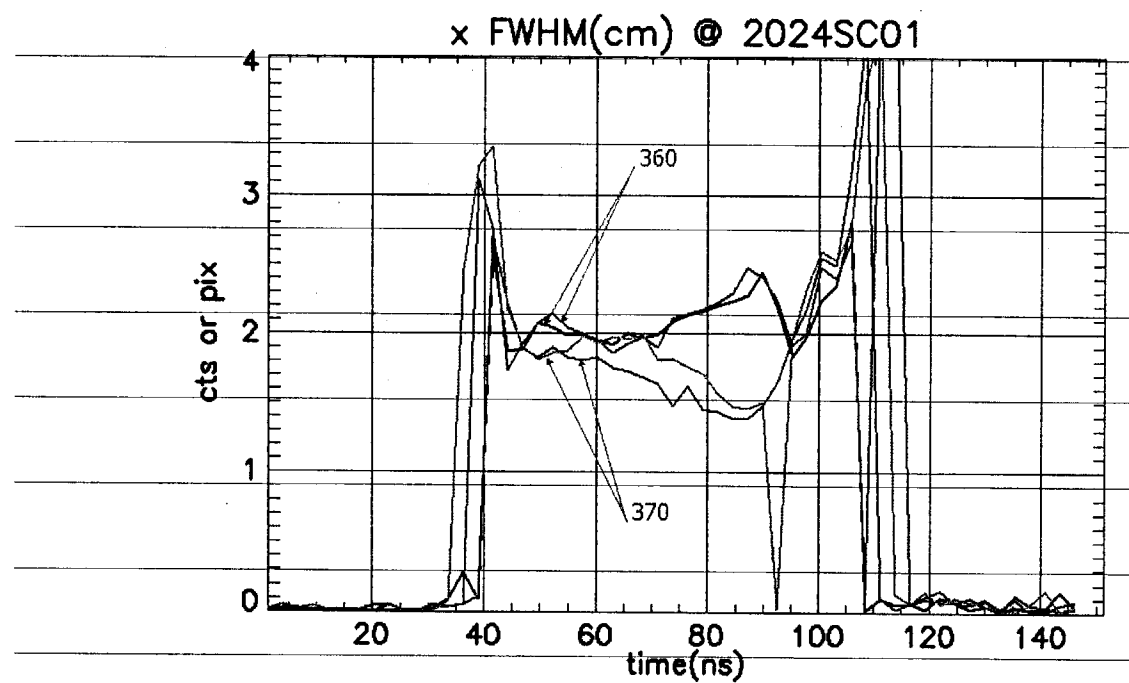


Fig 9 upstream: 3 mil graphite perpendicular to the beam  
downstream: 25 mil quartz with tungsten on us side, EF4=3 A

2024SC01 all a001

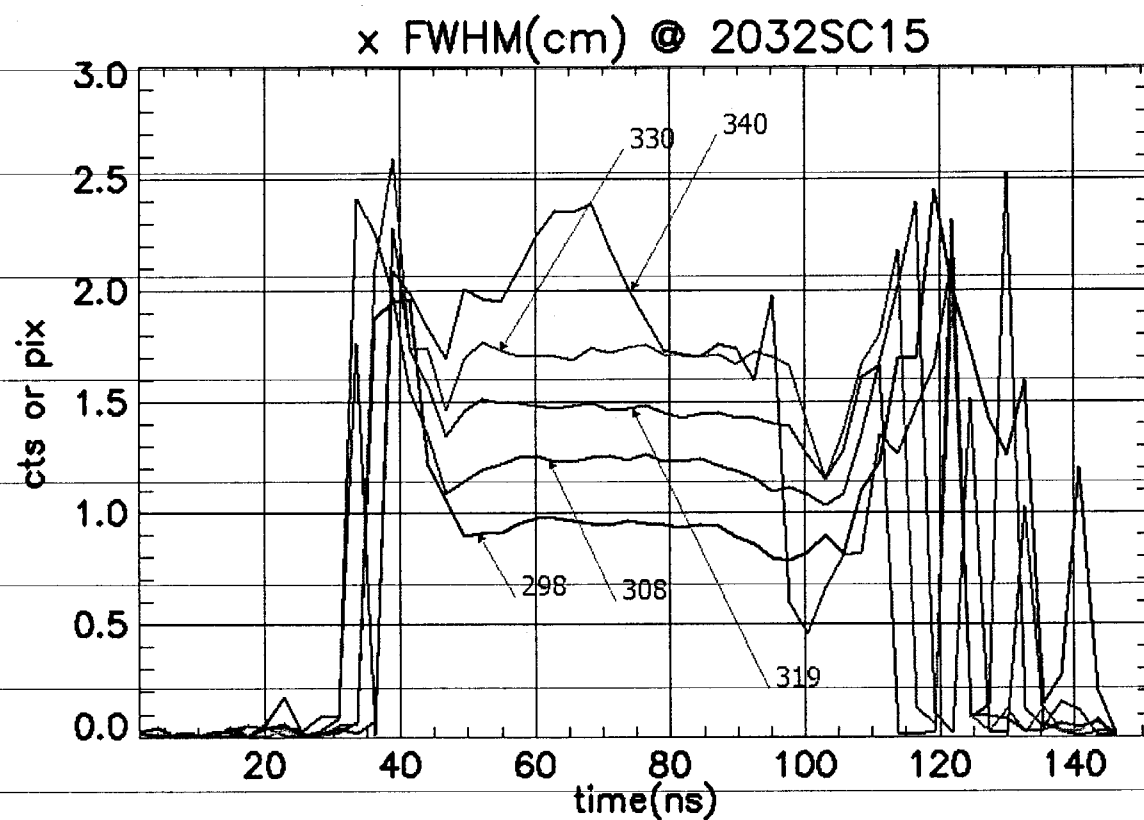


Fig 10 upstream: 0.5 mil mylar aluminized on ds side perpendicular to the beam  
downstream: 25 mil quartz with tungsten on us side

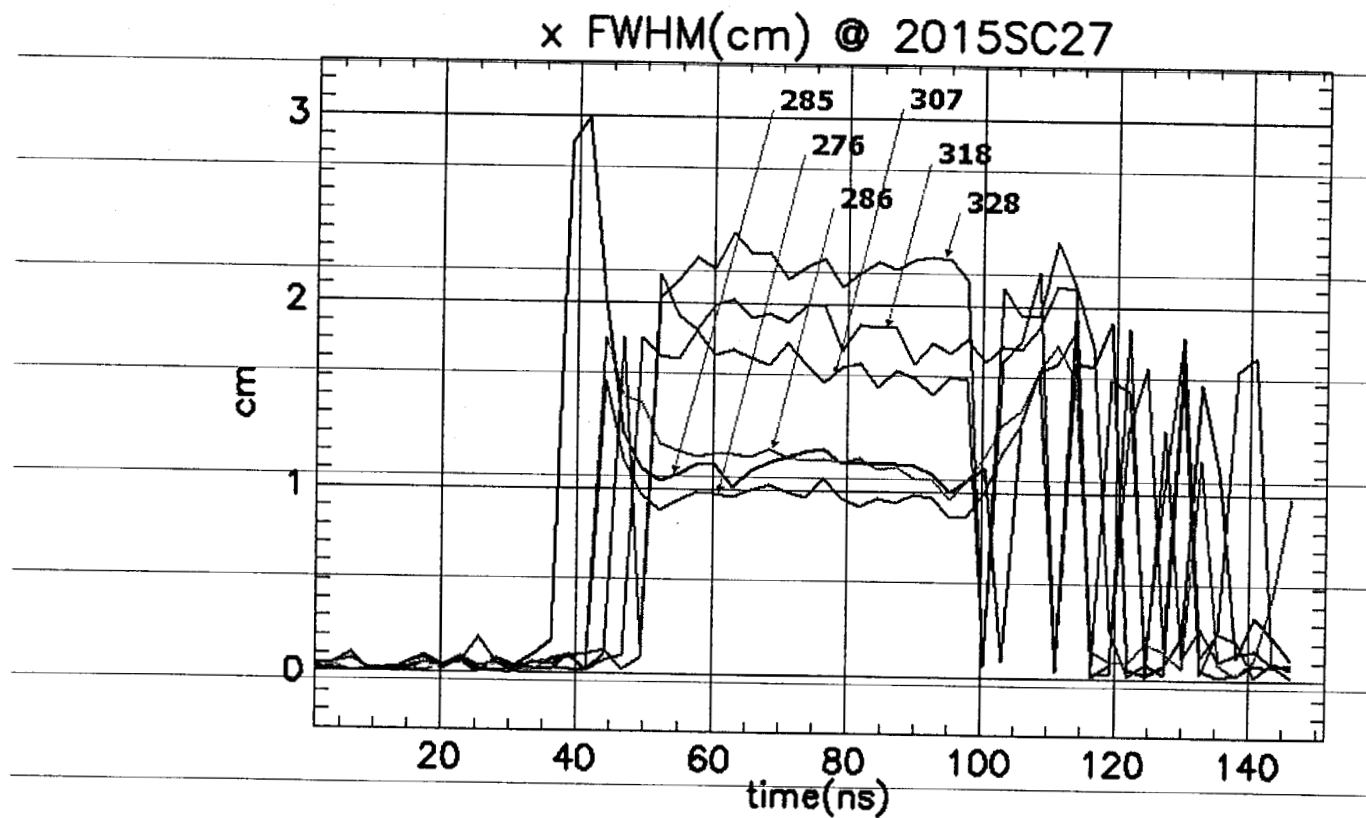


Fig 11 upstream: 0.5 mil mylar with aluminum on upstream side  
downstream: 0.5 mil mylar with aluminum on upstream side



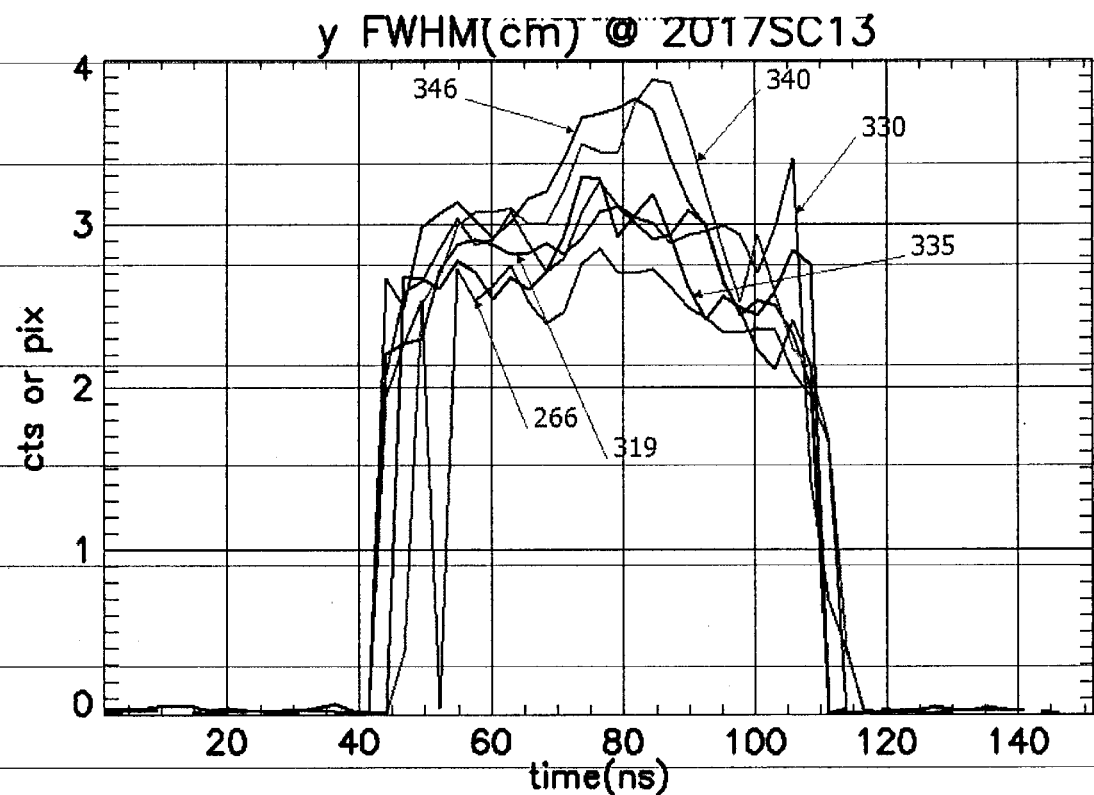


Fig 12 upstream: 3 mil tantulum perpendicular to the beam  
 downstream: 0.5 mil mylar with aluminum on us side, 15 X pressure increase

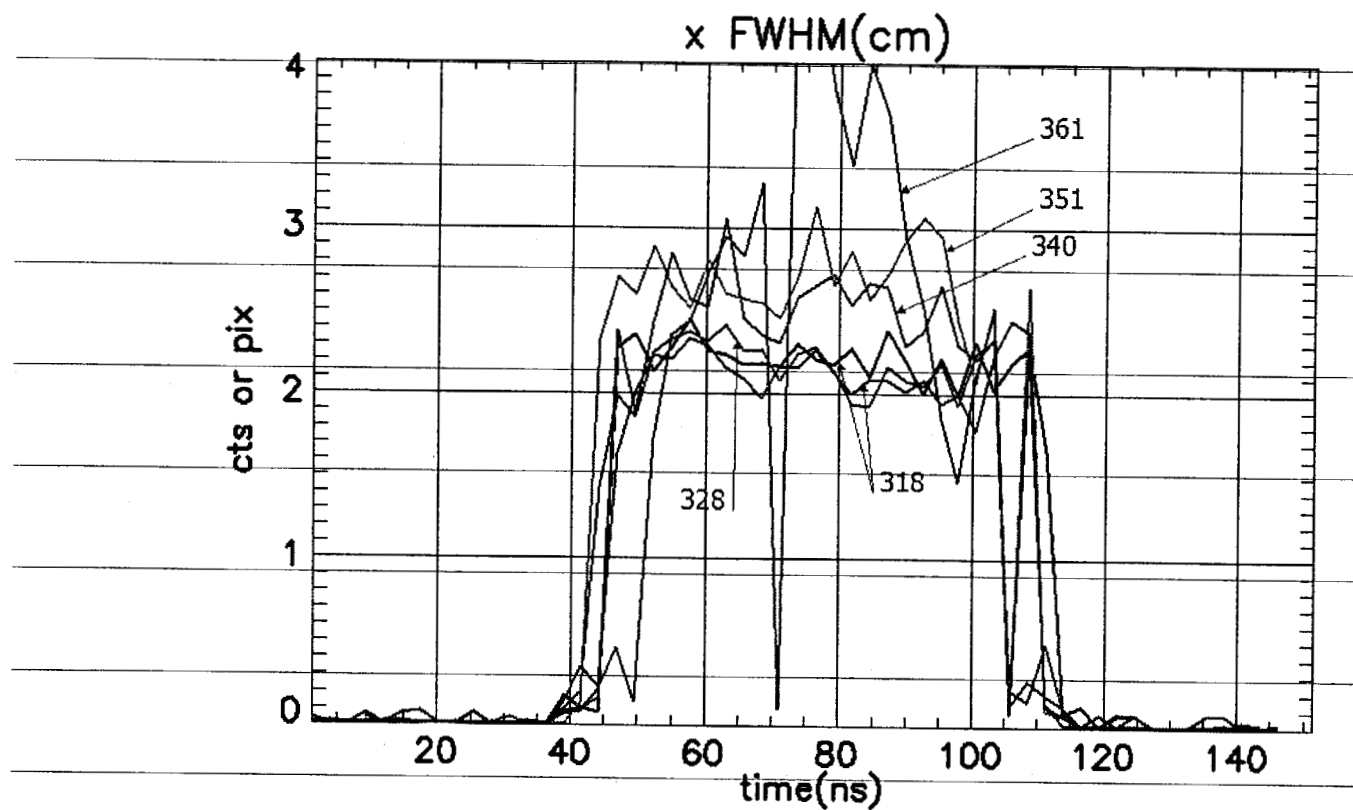


Fig 13 upstream: 0.5 mil stainless steel rotated 38 degrees from perpendicular  
downstream: 1 mil aluminum

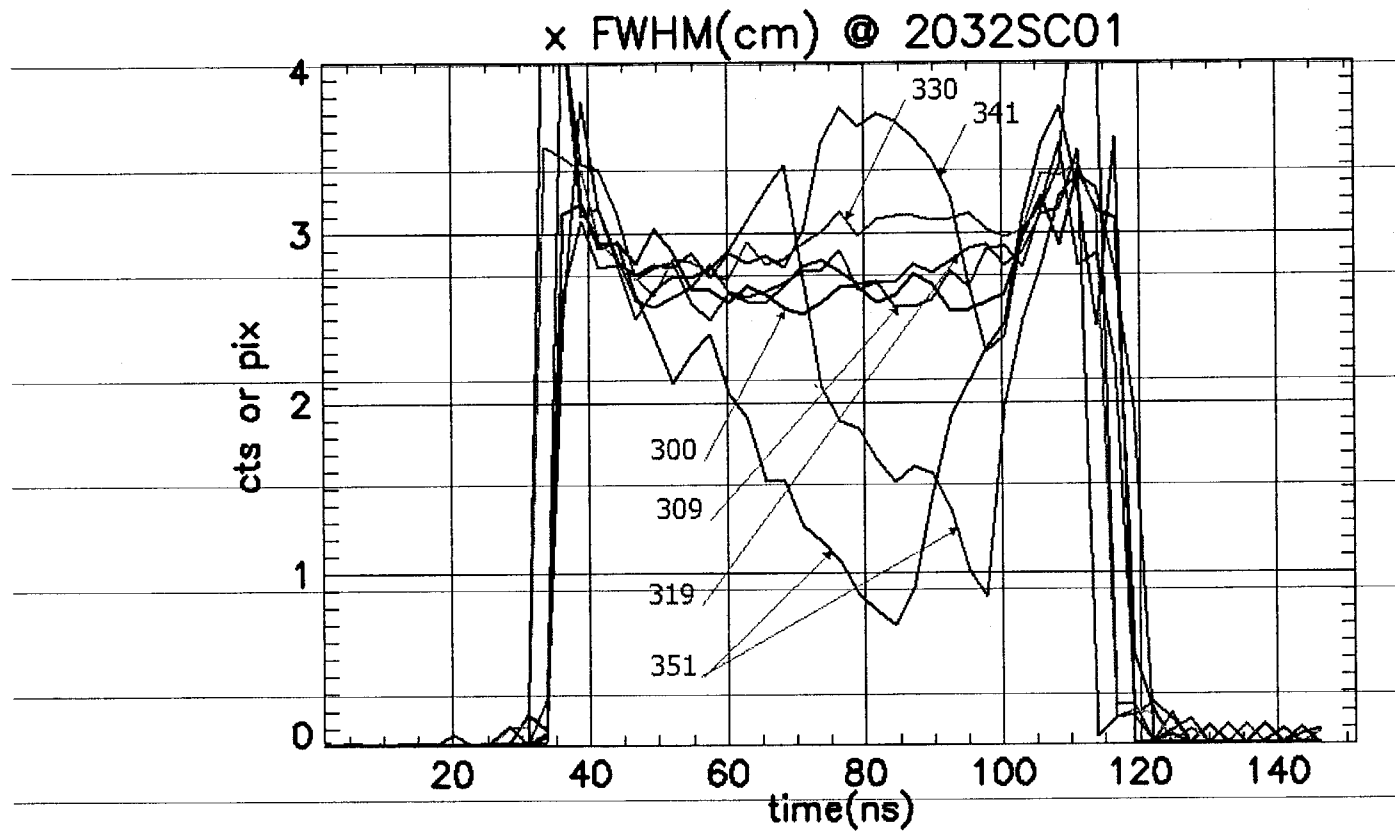


Fig 14 upstream: 0.3 mil tantalum perpendicular to the beam  
downstream: 25 mil quartz with tungsten on us side

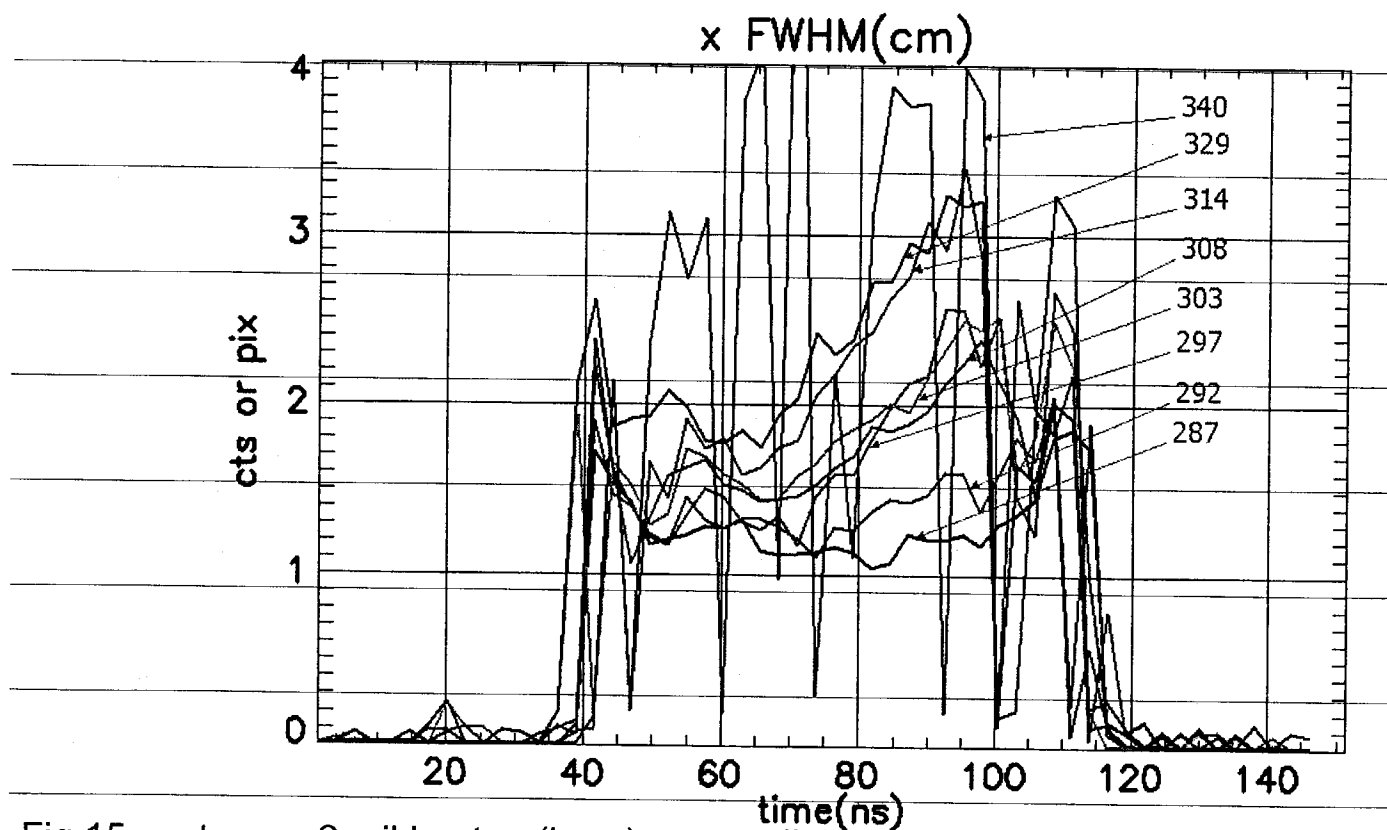


Fig 15 upstream: 2 mil kapton (bare) perpendicular to the beam  
downstream: 1 mil aluminum

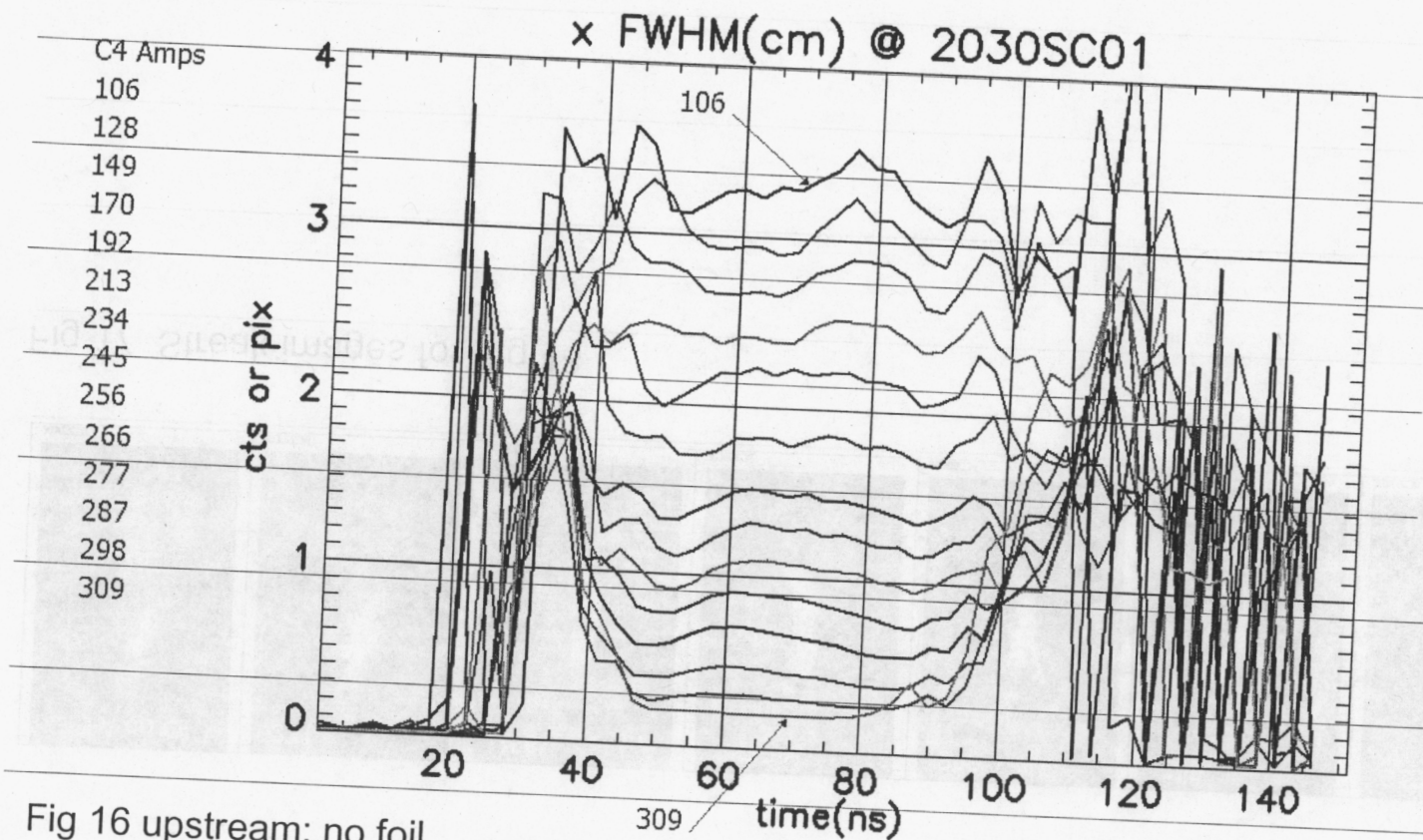


Fig 16 upstream: no foil

downstream: 25 mil quartz (bare), 3 mil graphite 1 cm upstream

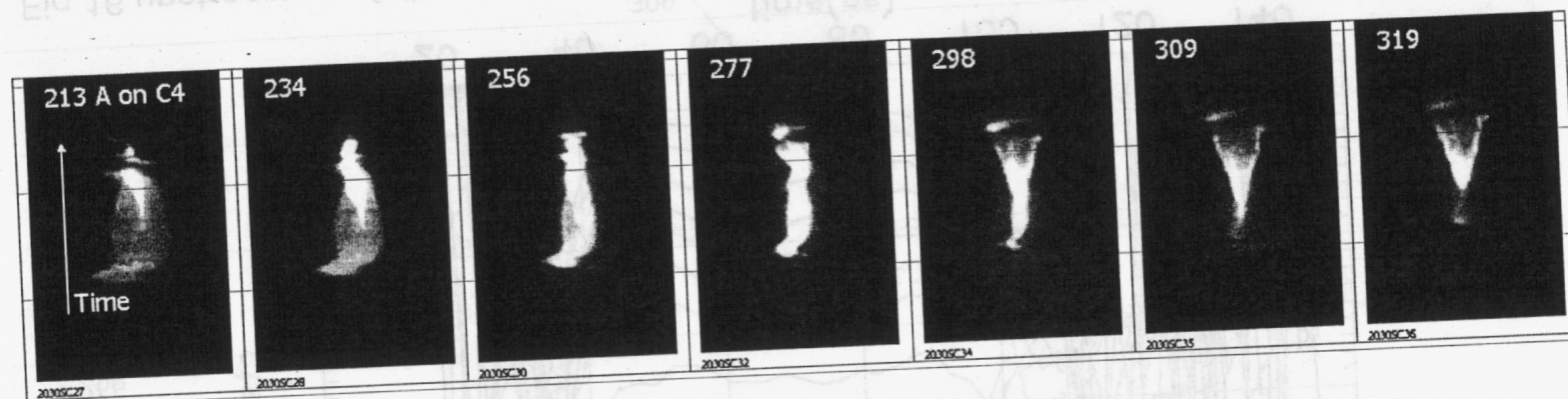


Fig 17 Streak images for Fig 18

File: 2030SC26 results 26to50.std

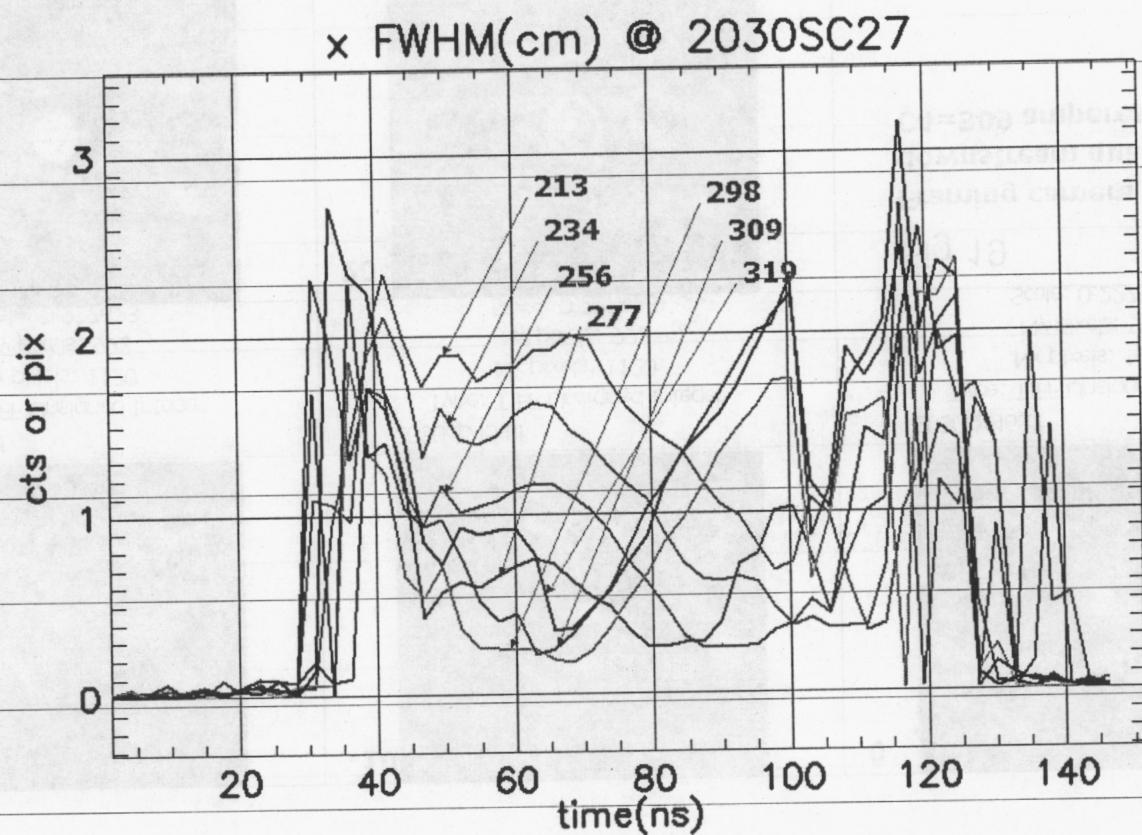
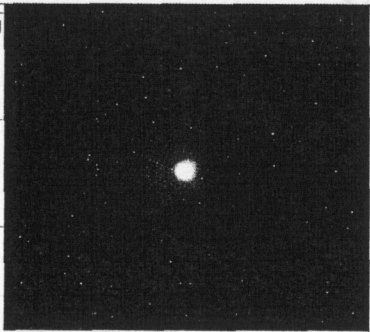

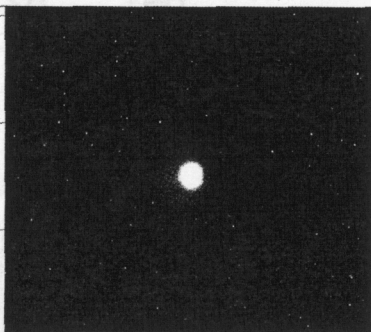
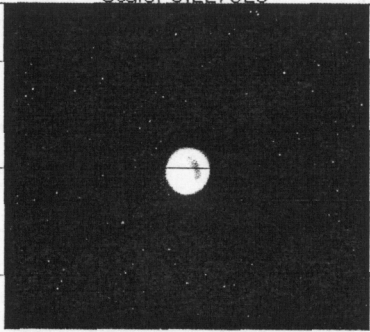
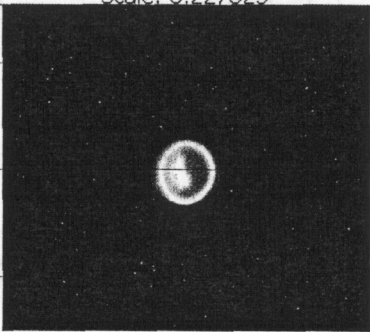


Fig 18 upstream: no foil

downstream: 25 mil quartz with no coating, no graphite foil



File: 2030dp44.tif

<b>-20</b> 	<b>-10</b> 	<b>0</b> 
2030dp44.tif Type: TIFF Unsigned Integer Nx pixels: 1120 Ny pixels: 992 Scale: 0.227823	2030dp45.tif Type: TIFF Unsigned Integer Nx pixels: 1120 Ny pixels: 992 Scale: 0.227823	2030dp46.tif Type: TIFF Unsigned Integer Nx pixels: 1120 Ny pixels: 992 Scale: 0.227823
<b>10</b> 	<b>20</b> 	<b>Fig 19</b> <b>Framing camera viewing</b> <b>downstream quartz plate</b> <b>C4=309 amperes</b>
2030dp47.tif Type: TIFF Unsigned Integer Nx pixels: 1120 Ny pixels: 992 Scale: 0.227823	2030dp48.tif Type: TIFF Unsigned Integer Nx pixels: 1120 Ny pixels: 992 Scale: 0.227823	



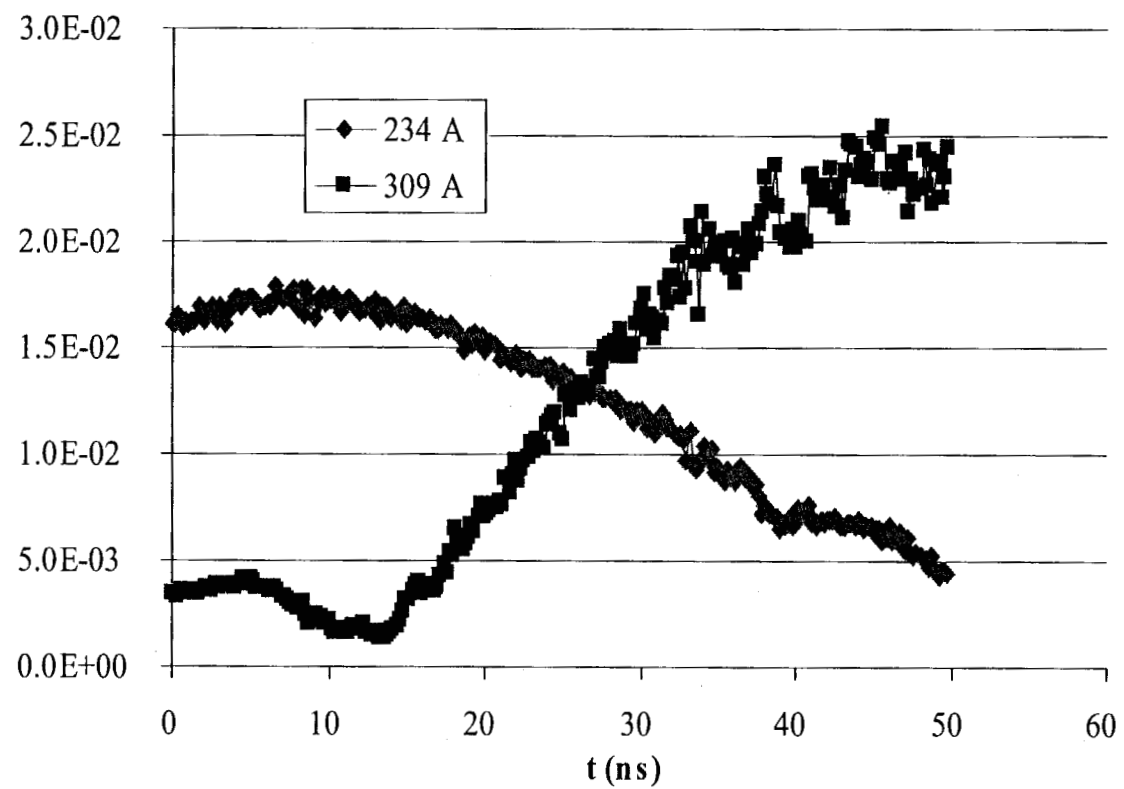


Fig 20 PIC calculations of beam radius (m) on quar target vs time, H+ ions

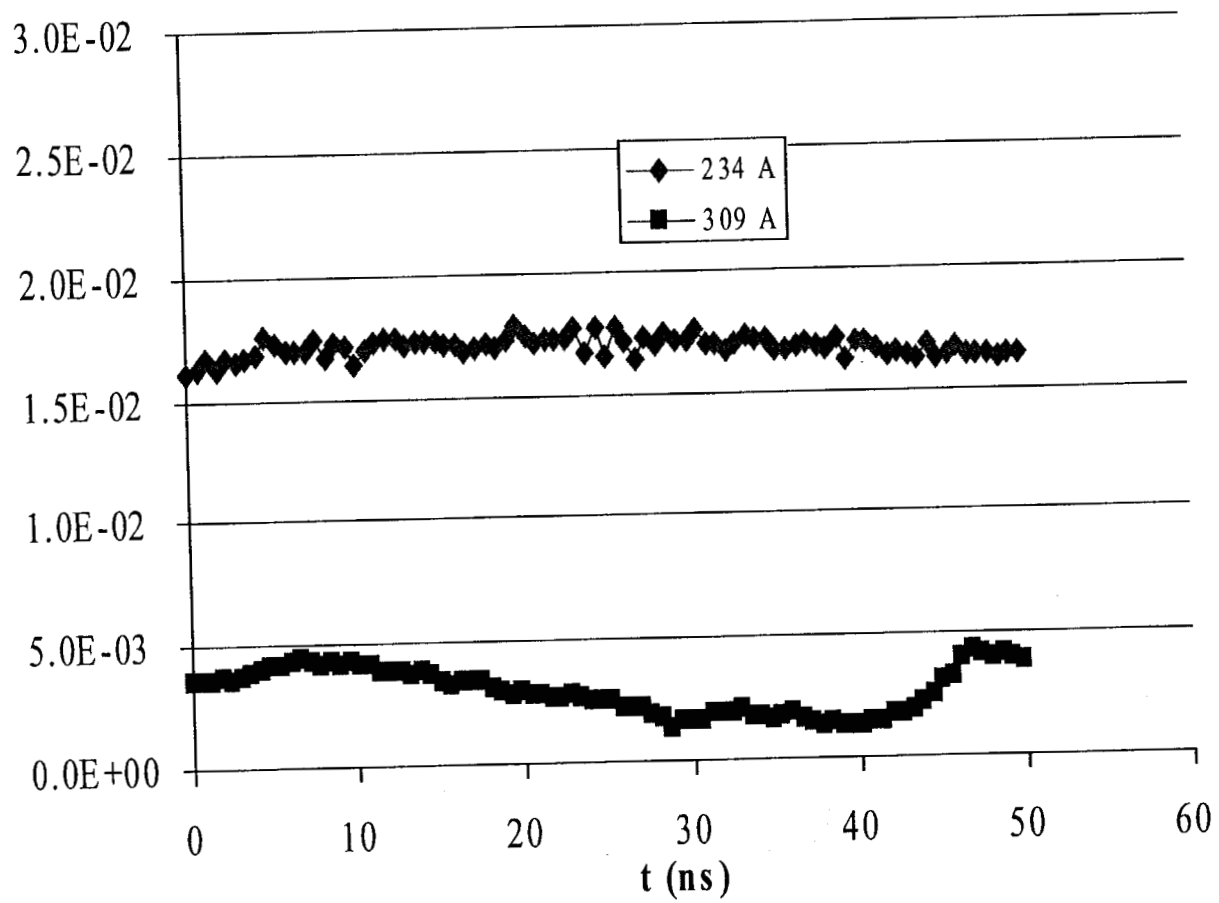


Fig 21 PIC calculations of beam radius (m) on quartz target vs time, C<sup>+</sup> ions

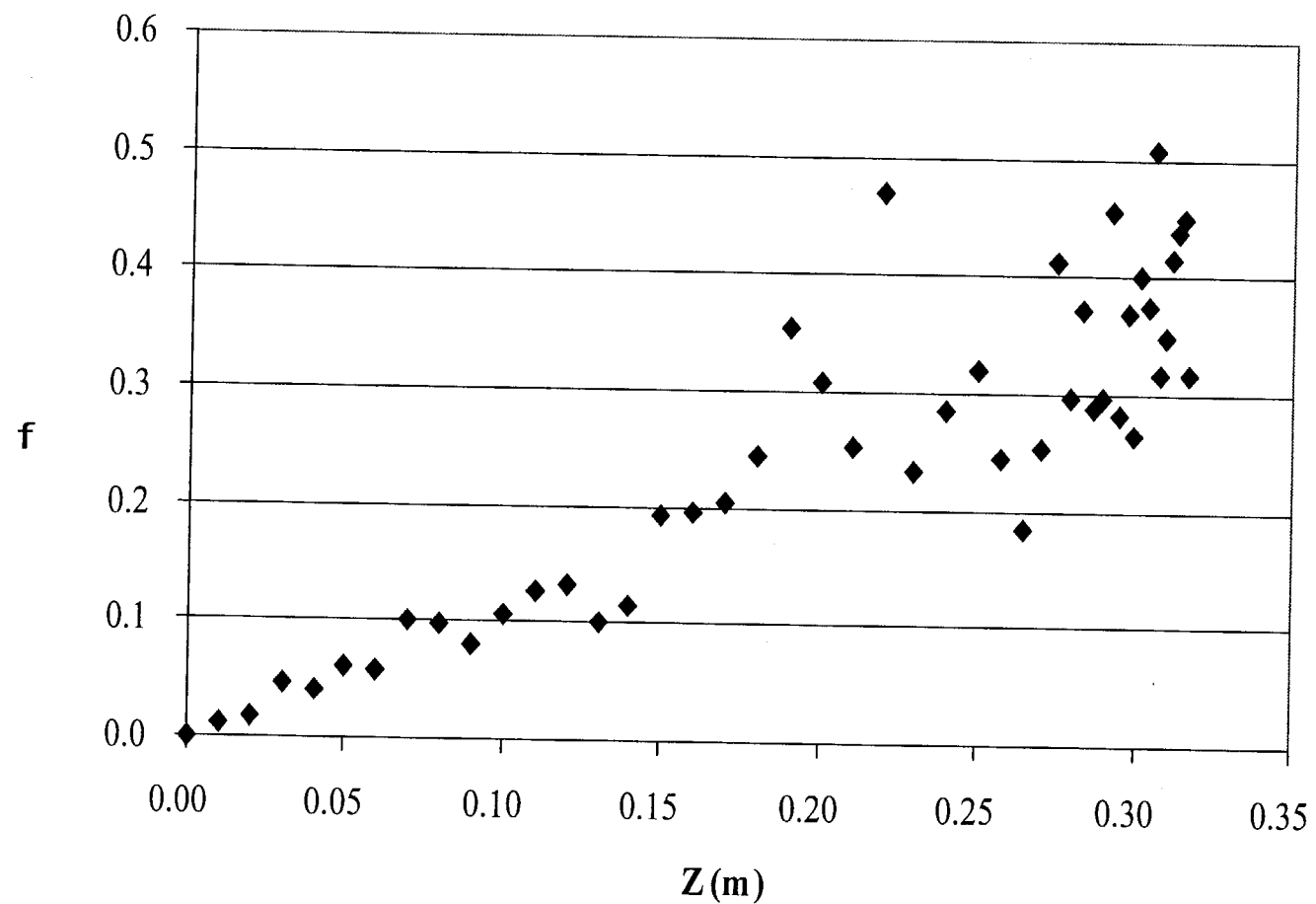


Fig 22 Electric field neutralization fraction  $f$  vs  $Z$ ,  
 $t=50$  ns,  $H=234$  A

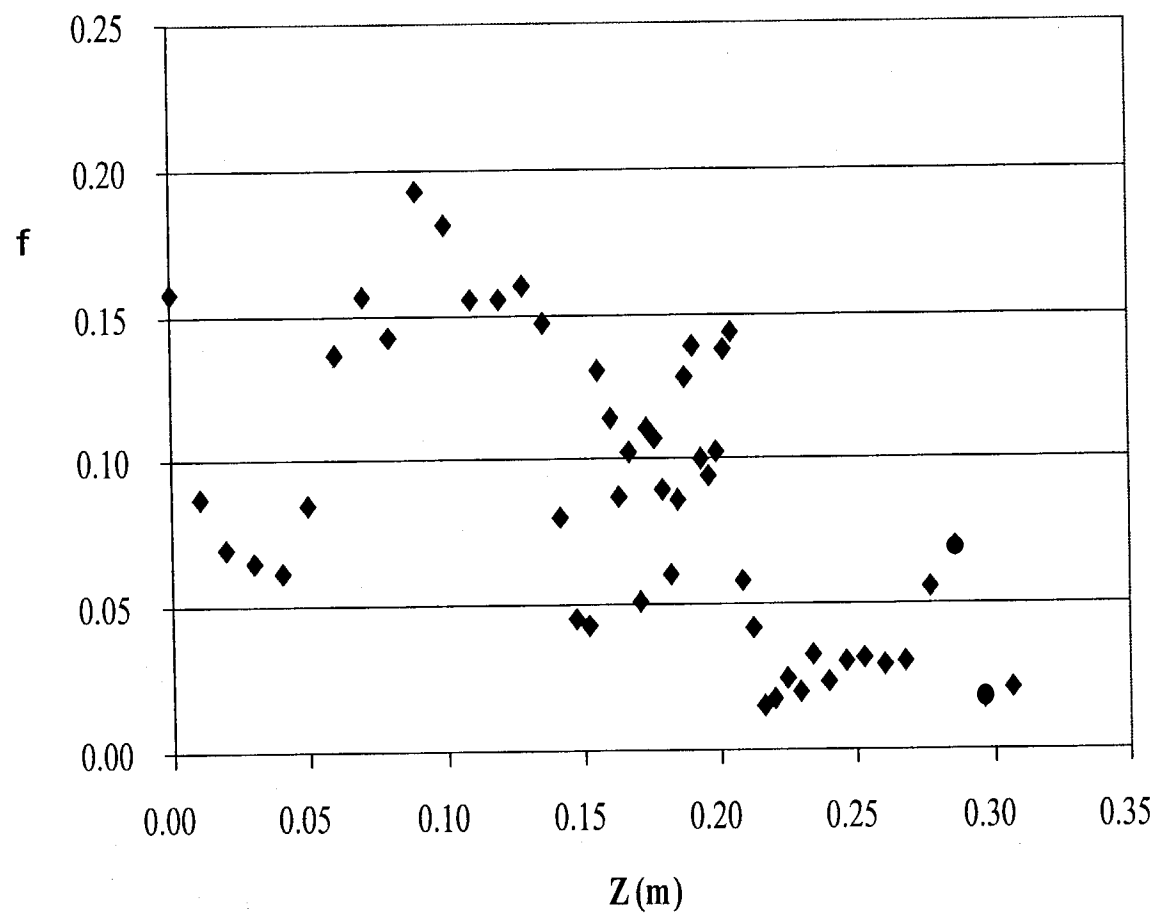


Fig 23 Electric field neutralization fraction  $f$  vs  $Z$ ,  
 $t=50$  ns,  $H^+$ ,  $C4= 309A$

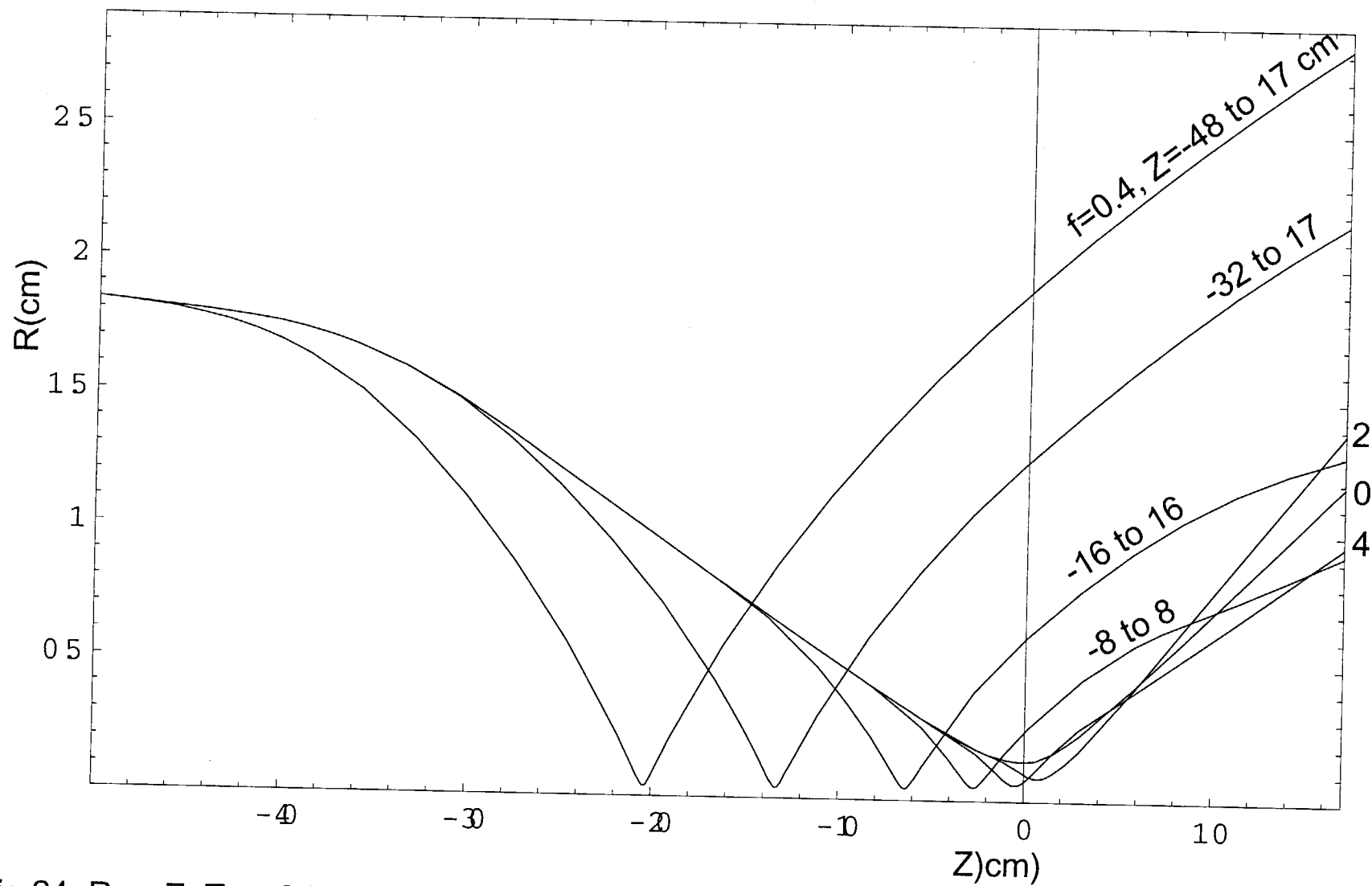


Fig 24, R vs Z, Two foil experiment with different lengths of rectangular f-column, 1 mil Alum

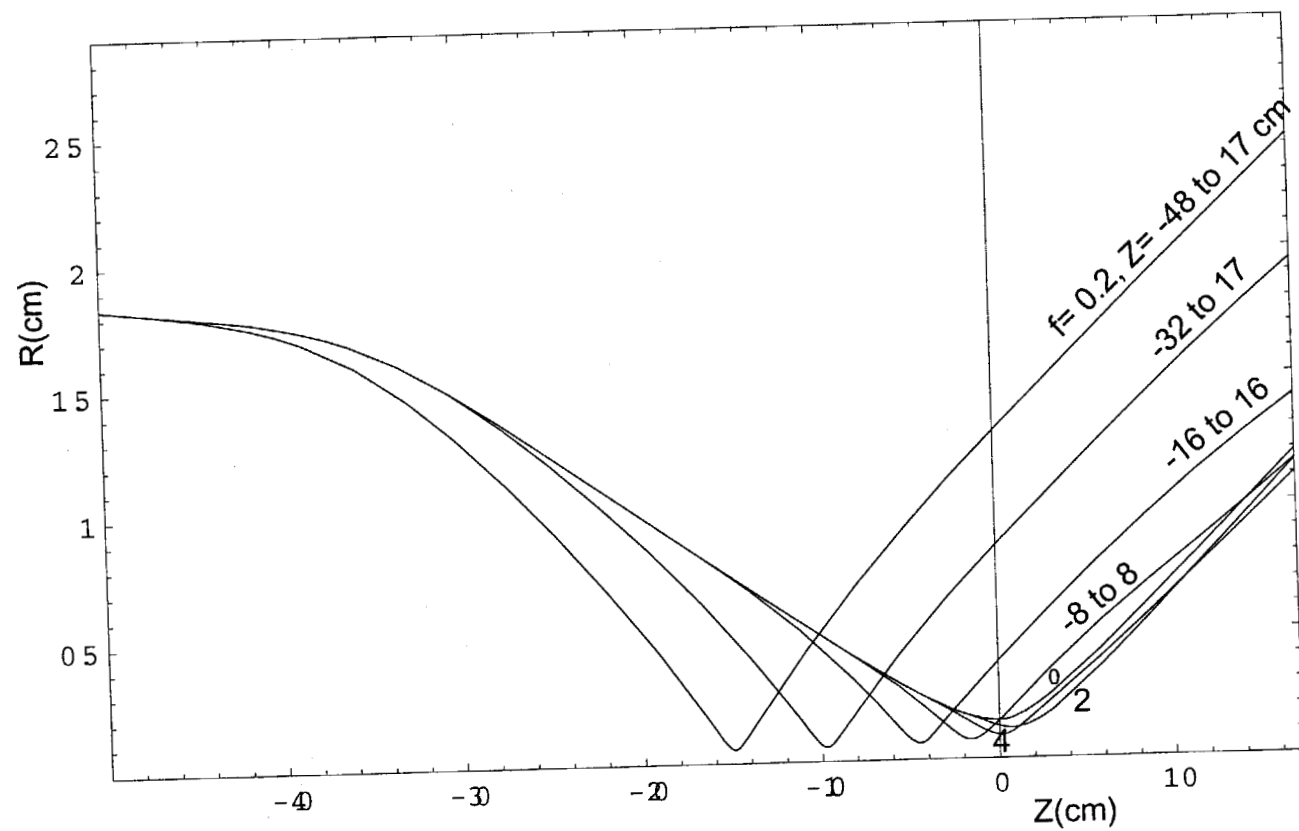


Fig 25,  $R$  vs  $Z$ , Two foil experiment with different lengths of rectangular  $f$ -column, 1mil Alurr

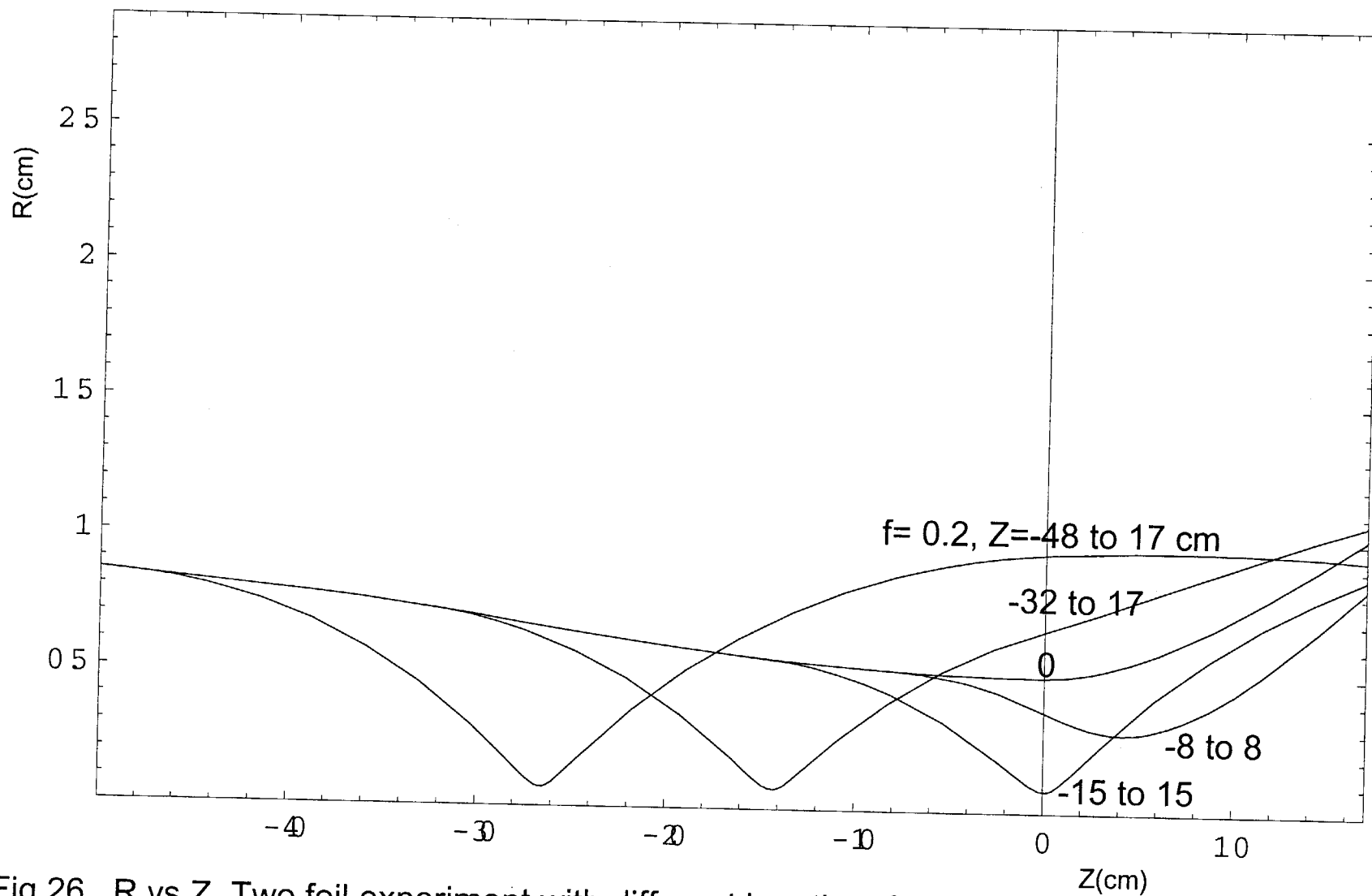


Fig 26,  $R$  vs  $Z$ , Two foil experiment with different lengths of rectangular f-column, 1 mil Alun

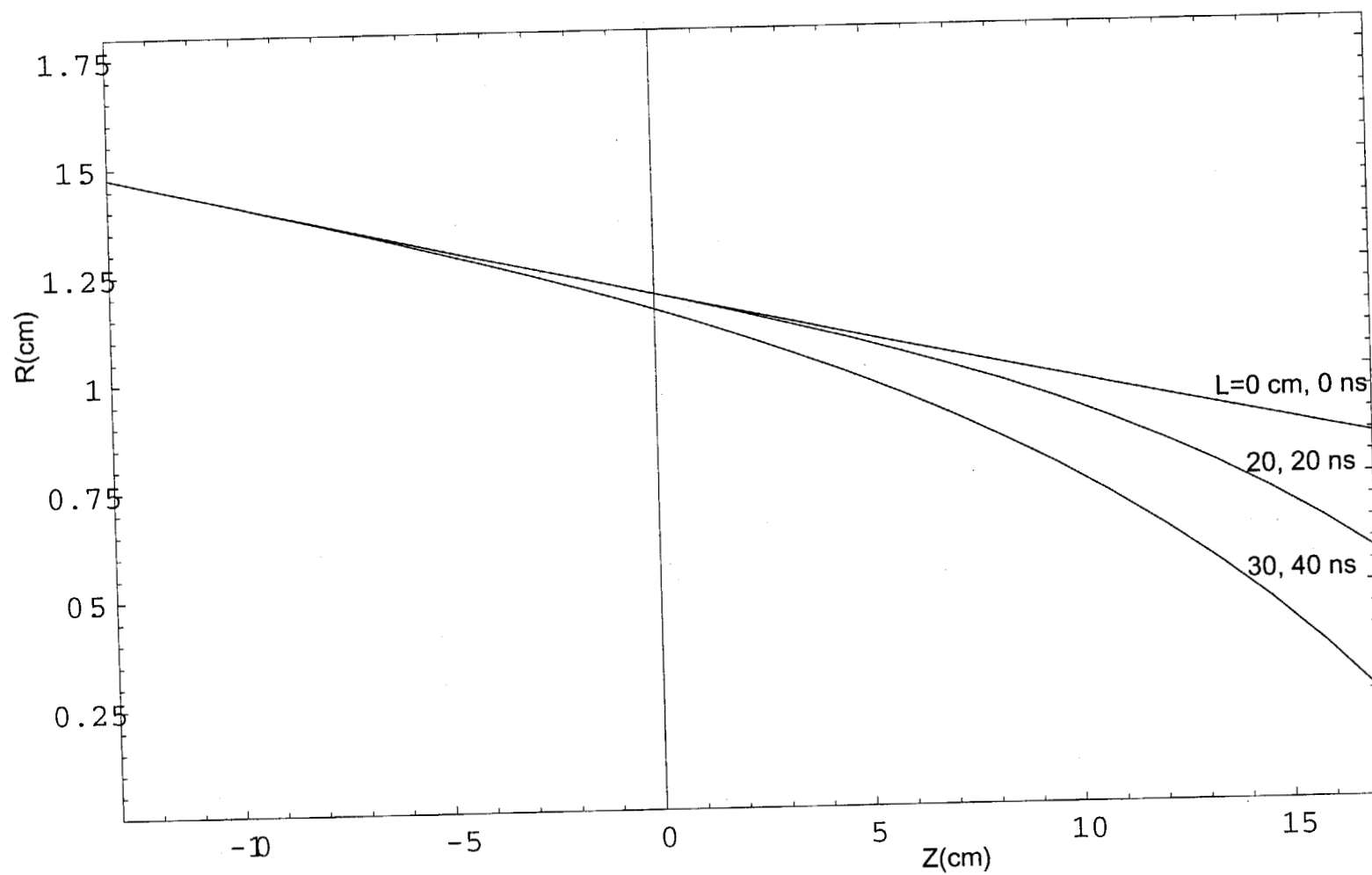


Fig 27, R vs Z, QUARTZ, C4=234A, f decreases linearly from 0.4 at the target to 0 at L cm upstream



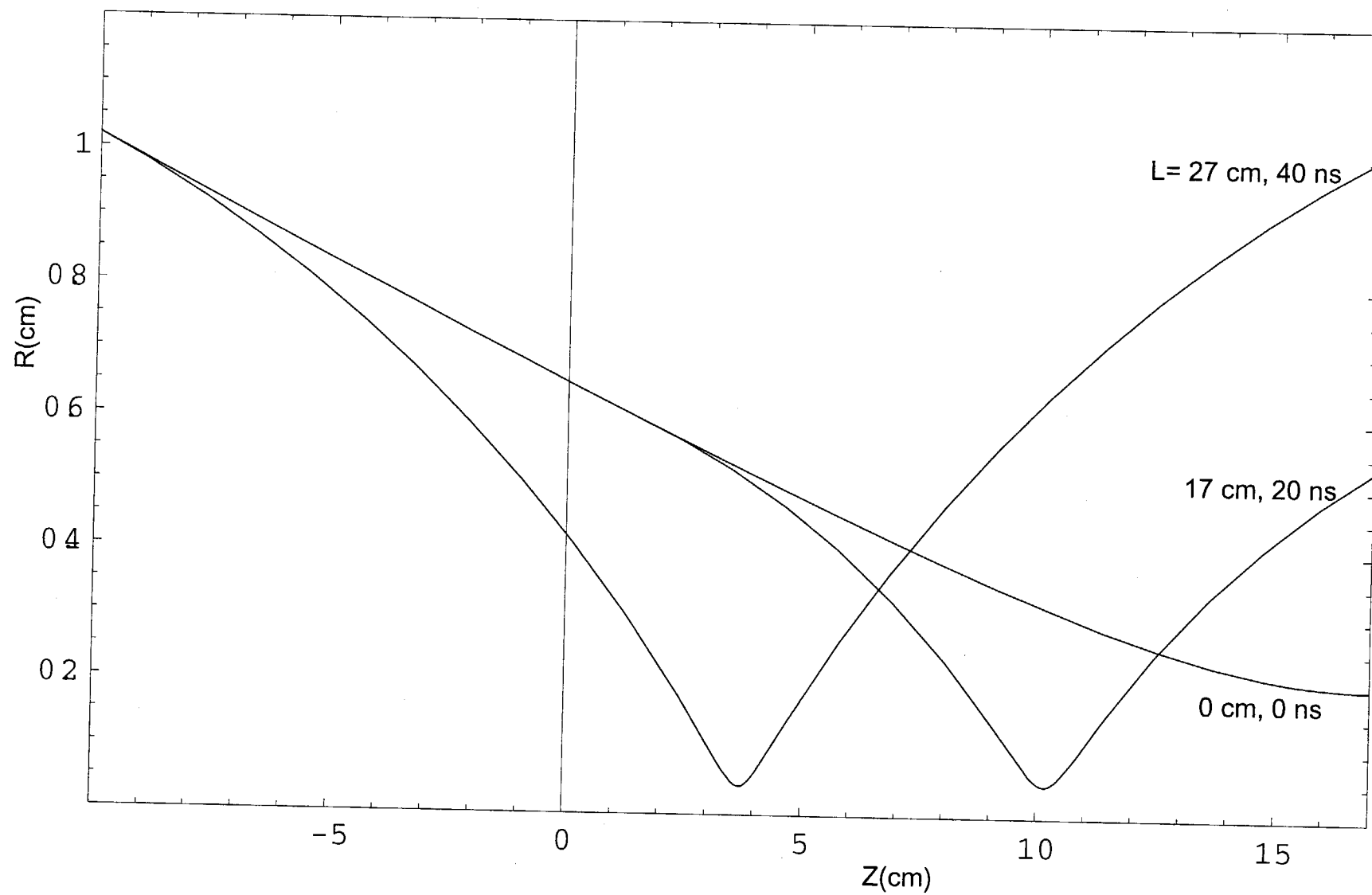


Fig 28, R vs Z, QUARTZ, C4= 309 A, f= 0.4 for L cm upstream of target

